Open Access

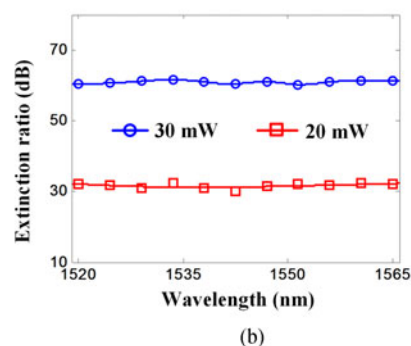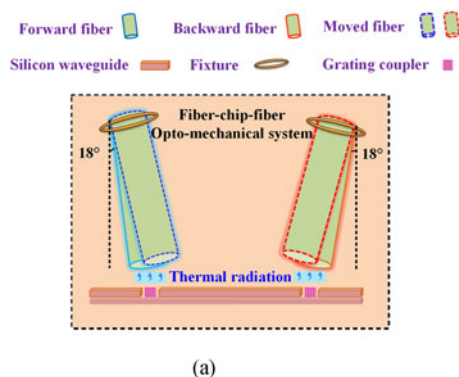# All-Optical Switch Based on a Fiber-Chip-Fiber Opto-Mechanical System With Ultrahigh Extinction Ratio

Li Liu
Jin Yue
Zhihua Li

IEEE

All-Optical Switch Based on a Fiber-Chip-Fiber Opto-Mechanical System With Ultrahigh Extinction Ratio

Li Liu,[1,2] **Jin Yue,**[3] **and Zhihua Li**[1,2]

[1]School of Automation, China University of Geosciences, Wuhan 430074, China
[2]Hubei key Laboratory of Advanced Control and Intelligent Automation for Complex Systems, Wuhan 430074, China
[3]Wuhan National Laboratory for Optoelectronics & School of Optical and Electrical Information, Huazhong University of Science and Technology, Wuhan 430074, China

Abstract: We propose and experimentally demonstrate an all-optical switch based on a fiber-chip-fiber opto-mechanical system driven by thermal radiation. The two optical fibers are both designed as movable cantilever structures with a free-hanging length. With injecting pump lights into the opto-mechanical system, the generated thermal radiation between the grating couplers and the optical fibers could effectively move the fibers with displacements up to tens of micrometers. Thus, the optical fibers would completely deviate from the corresponding grating coupler to cut off the optical signal transmission. In the experiment, using light to control light, both ultrahigh switching extinction ratios beyond 60 dB and an operation bandwidth of at least 45 nm have been achieved by taking advantage of the powerful thermal radiation. To the best of our knowledge, this is a record extinction ratio for fiber-based all-optical switch. The significant thermal radiation opens up a new opportunity and solution for all-optical switch. In the future, the significant effect is promising to be used in fully integrated chips to greatly reduce the required pump power. Moreover, the proposed device has many other applications in all-optical systems, such as reconfigurable logic gates.

Index Terms: All-optical switch, opto-mechanical system, thermal radiation, ultra-high switching extinction ratio.

1. Introduction

Optical devices which could control the on-off states of optical transmissions are a fundamental research and long-standing goal in optical communication networks [1]–[3]. In particular, all-optical switches are key devices in which one light beam could efficiently control another [4]–[6]. If integrated with modern fiber-optical technologies, such devices have important applications for optical communication and computation in telecommunication networks [7]. In the past decade, the fiber nonlinear effects and interactions between fibers and light have been attracted great interests for their advantages of high efficiency and tunability [8]–[12]. To pursue better switching performance and lower cost, different all-optical switches have been demonstrated using fiber-based
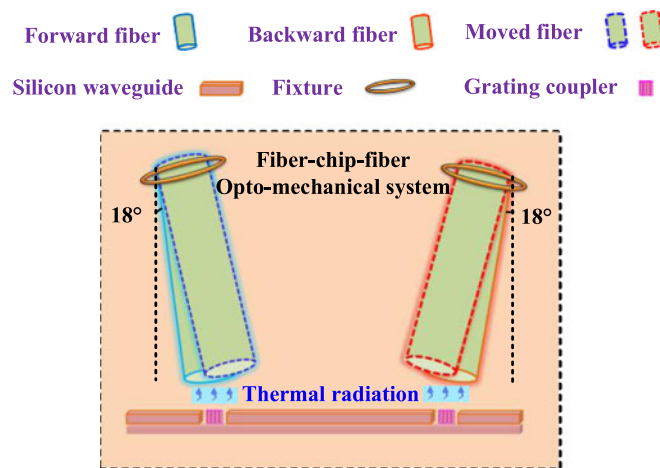
Fig. 1. Schematic diagram of the fiber-chip-fiber opto-mechanical system.

nonlinear effects, including slow light [4], thermo-optic effect [13], bend effect [14], pulse trapping [15], phase-sensitive amplifier [16], Kerr effect [17], cross-phase modulation [18] and so on [19]–[23]. For all-optical switches, one primary requirement is high switching extinction ratio. High-sensitive optical systems (such as high-precision optical measurement and sensor devices) require to be completely separated from unwanted interference and noise. In these cases, any unwanted light should be eliminated as possible when the optical path is cut-off, namely ultra-high switching extinction ratios are required [24]. However, to date, most reported schemes are limited in extinction ratios (such as 33 dB in [13], 15 dB in [14], 30.4 dB in [16] and 26 dB in [25]). Few schemes of all-optical switch have achieved high extinction ratios beyond 60 dB. In order to break this limitation, an effective mechanism for all-optical switch is highly desired to realize high extinction ratios.

According to Kirchhoff's radiation law, any practical objects would constantly emit thermal radiations into the surrounding space [26], [27]. The higher temperature the objects have, the stronger thermal radiation would emit. Especially, the thermal radiation has high directivity during the energy transformations [28]–[30]. Compared with optical gradient force [31]–[33] and optical radiative force [34]–[36], the thermal radiation is more drastic and could offer an alternative solution enabling all-optical control in optical communication systems to effectively process signals.

In this paper, we experimentally investigate and demonstrate for the first time all-optical switch with ultra-high extinction ratios based on a fiber-chip-fiber opto-mechanical system. By using the novel phenomenon of fiber movements driven by thermal radiation, the experiment results show an ultra-high extinction ratios beyond 60 dB and a relatively broad operation bandwidth of 45 nm. To the best of our knowledge, this is a record switching extinction ratio in fiber-based all-optical systems. Moreover, the proposed scheme might have other significant applications in all-optical communication systems, such as reconfigurable logic gates.

2. Operation Principle

As shown in Fig. 1, the fiber-chip-fiber opto-mechanical system consists of a silicon straight waveguide and a pair of single-mode fibers. The diameter of the fiber core is 10 μm. The two fibers are both designed as movable cantilever structures with a free-hanging length and tilted at an angle of 18°. The operation principle of the all-optical switch is based on the light-matter interaction. It is well known that absorption of photons by solid structures would result in temperature changes and thermal expansion [37], which has significant applications for signal processing. For instance, a pump light with high power and a signal light with low power are injected into the forward fiber together. It should be noted that the wavelength of pump light is out of the working bandwidth of the silicon grating couplers while the signal light could couple into the grating with high efficiency. Major
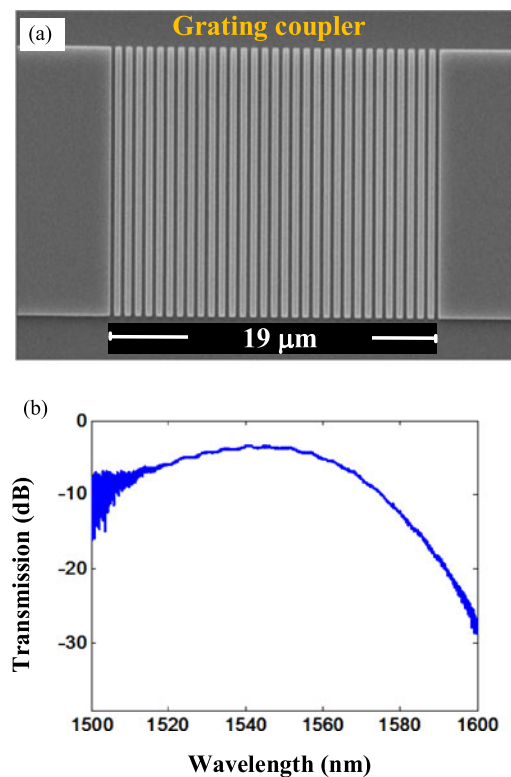
Fig. 2. (a) SEM image of the grating coupler. (b) Measured transmission response of the silicon chip.

pump power would be scattered at the grating due to the low coupling efficiency between the fiber and the grating coupler. Thus the grating temperature is rapidly increased which results a thermal gradient between the grating and its surroundings. Then, as the lower side of fiber would absorb the infrared powers emitted by the hot grating coupler, it is hotter than the fiber upper side. With injecting pump light with milliwatt power level into the device, the infrared power absorbed by the fiber is only a small percentage of pump power [38]. The temperature values of the grating coupler, differences between the lower and upper side of the fiber are tens of degree centigrade [39], [40]. Due to the thermal non-equilibrium, the fiber would be deformed and deviate a displacement from the grating coupler. The fiber deformation is related to the power of the incident pump light as well as the optical, mechanical and thermal properties of the fiber cantilever. In this case, the signal transmission would be cut off. Moreover, the backward fiber could be simultaneously manipulated by a backward pump light to double the switching extinction ratios. Therefore, in the proposed all-optical switch, without pump powers the signal light could transmit though this system with low-loss. Once injecting pump lights into the fibers, the signal transmission would be blocked due to the fiber movement driven by the fiber thermal expansions.

The silicon device is fabricated on a commercial silicon-on-insulator (SOI) wafer whose top silicon thickness and buried oxide layer thickness are 340 nm and 2 μm, respectively. The device layout is transferred to a ZEP520A photoresist using E-beam lithography. Then, the upper silicon layer is etched downward of 245 nm to form a ridge waveguide through inductively coupled plasma (ICP) etching. The scanning electron microscope (SEM) image of the grating coupler is shown as Fig. 2(a). The period, duty cycle and total length of the grating are 623 nm, 58% and 19 μm, respectively. Fig. 2(b) shows the measured transmission response of the silicon chip, indicating an insertion loss of 3.5 dB. The 3-dB bandwidth of the grating coupler is 45 nm, ranging from 1520 nm to 1565 nm. The wavelength of pump light is chosen as 1600 nm with 14.5 dB single-side coupling loss to induce strong scattered pump powers at the gratings.
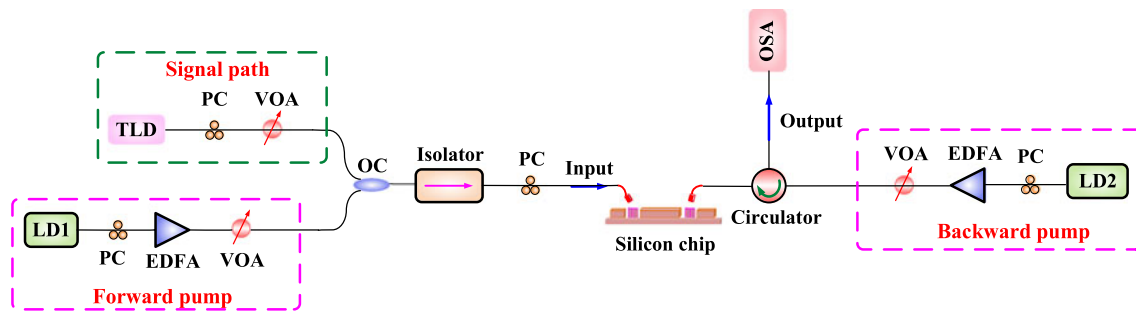
Fig. 3. Schematic illustration of the experimental setup. LD: laser diode, PC: polarization controller, EDFA: erbium-doped fiber amplifier, VOA: variable optical attenuator, TLD: tunable laser diode, OC: optical coupler, OSA: optical spectrum analyzer.
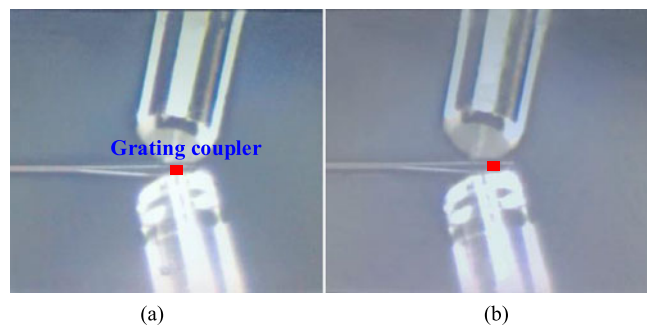

(a)   (b)

Fig. 4. CCD images of the backward fiber. (a) Initial state. (b) With injecting pump power of 25 mW.

3. Experimental Results

In order to verify the theoretical analysis, we carry out experiments with the configuration as shown in Fig. 3. The wavelength of the continuous-wave (CW) lights emitted from the two laser diodes (LD1 and LD2) are both fixed at 1600 nm. After amplified by the followed erbium-doped fiber amplifiers (EDFAs), the forward and backward pump lights in the pink boxes are injected into the corresponding fiber. The wavelength of the signal light emitted from the tunable laser diode (TLD) is tuned ranging from 1520 to 1565 nm. Then the signal light transmits into the silicon chip and passes though the circulator. Finally, the output power of the signal light is measured by the optical spectrum analyzer (OSA) in order to characterize the switching performances.

The free-hanging lengths of the two fibers are both set at 2.1 cm. Fig. 4 shows the charge coupled device (CCD) images of the backward fiber. At first, the backward fiber is accurately aligned with the grating coupler (marked as the red box), as shown in Fig. 4(a). As the length of the grating coupler is unequivocal (i.e. 19 μm) which could be used as the benchmark, the fiber displacements could be calculated through the scale conversions in the CCD images. Once injecting a pump power of 25 mW, the backward fiber deviates a distance of 13 μm from the grating coupler, as shown in Fig. 4(b).

To further explore the relationship between the input pump power and the fiber moving displacement, the backward pump power is tuned ranging from 15 to 30 mW, shown as the blue line in Fig. 5. When a backward pump power of 30 mW is injected, the fiber could move a displacement of 21.6 μm which is larger than the grating length. Namely, the fiber completely deviates from the grating which leads to high coupling loss of the signal light. Considering the material characteristics and displacement magnitude, the fiber movement could be mainly attributed to the thermal expansion [41]–[43]. Subsequently, a forward pump light (the same power as the backward pump light) and a signal light (fixed at wavelength of 1550 nm and power of 0.1 mW) are coupled together and injected into the forward fiber. In this case, the extinction ratios of the all-optical switch have
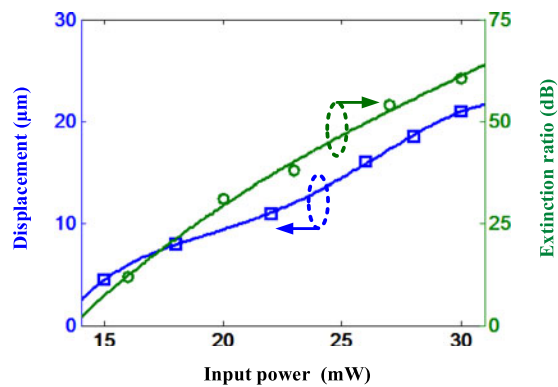
Fig. 5. The displacements of the backward fiber and extinction ratios of the all-optical switch under different pump powers.
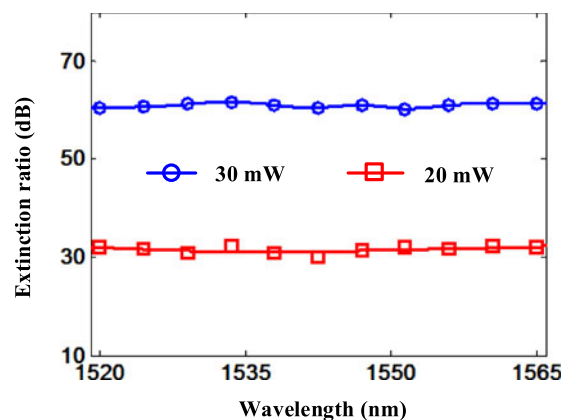

Fig. 6. The bandwidths of the all-optical switch under different pump powers.

been measured, shown as the green line in Fig. 5, which is increased with the input pump powers. When two pump powers of 30 mW are injected into the corresponding fiber, the maximum switching extinction ratio could be up to 60.7 dB. And the extinction ratios are tunable according to the pump power levels.

Subsequently, the forward and backward pump powers are both fixed at 20 mW to investigate the switching bandwidth. The input signal wavelength is tuned ranging from 1520 to 1565 nm (in the 3-dB bandwidth of the grating coupler). The extinction ratios of the switch are all larger than 30 dB, shown as the red line in Fig. 6. Finally, the two pump powers are both increased to 30 mW in order to induce stronger thermal radiation and larger fiber displacements. The switching extinction ratios significantly increase beyond 60 dB indicating a switching bandwidth of at least 45 nm, shown as the blue line in Fig. 6. In the future, by using a grating coupler with much wider 3-dB bandwidth, the bandwidth of the proposed switch could be greatly increased.

The response speed of the switch is limited by the intrinsic characteristic of fiber mechanical effect. When the two pump powers are set at 30 mW, the 10–90% rise time and fall time are measured as 86 and 75 ms, respectively. Moreover, we have investigated the fiber return movement by removing the pump light. Initially, the two fibers are aligned with each corresponding grating coupler. With injecting signal light with 1 mW power at 1550 nm into the forward fiber, the output power of the backward fiber is measured as 0.32 mW. Subsequently, a pump power of 30 mW is injected into the forward fiber to cut off the signal transmission. Once the pump power is turned off, the forward fiber could move back to the corresponding grating coupler. In this case, the output signal power is
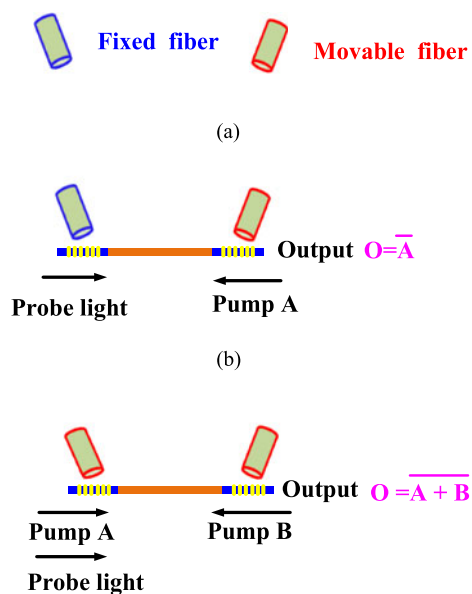
Fig. 7. Structures of the reconfigurable all-optical logic gates. (a) NOT gate. (b) NOR gate. The output probe power is marked as "O".

measured as 0.27 mW. Therefore, when the pump power is cut off, the deformed fiber is competent to align with the grating coupler again.

In the future, the fiber structure could be specially designed in order to reduce the fiber weight, such as by optimizing the diameter of the fiber claddings. In this case, the resistance could be decreased, which contributes to reduce the pump powers. Moreover, the powerful thermal radiation could be used in fully on-chip devices for large-scale integration which is promising to greatly reduce the pump power. The switching function of the free-hanging fibers could be instead of improved devices using more light and compact materials, such as movable cantilever waveguides in SOI platform [44]–[46]. As the weight of the on-chip movable counterpart is much lighter than the fiber, the SOI system is more efficient to convert the scattered light power to the fiber mechanical energy. Thus the required pump power might be greatly reduced as several milliwatts. The insertion loss of the proposed switch could be reduced to 0.58 dB and the operation bandwidth could increase to 80 nm by using the ultra-low loss grating couplers [47].

Except for all-optical switch, the proposed system based on the thermal radiation could be also used to realize all-optical reconfigurable logic gates. As an example, a NOT gate and a NOR gate have been designed respectively. It should be noted that the pump light (high power) is also out of the working bandwidth of the grating coupler in order to induce strong scattering, while the probe light (low power) could couple into the device with high efficiency. Initially, the fibers are aligned with each corresponding grating coupler. Fig. 7(a) presents a NOT gate consisting of two fibers with the left one fixed and the other movable. Once a pump light (Pump A) is injected into the right fiber (i.e. A = 1), the movable right fiber would deviate away from the grating coupler, thus the probe light injected from the left fiber could not arrive at the output port. The output probe power is marked as 'O' and in this case O = 0. On the other hand, when there was no incident pump light (i.e. A = 0), the probe light could approach full output (i.e. O = 1). Hence, the NOT gate is successfully realized. As shown in Fig. 7(b), the NOR gate can also be obtained by using two movable fibers. Only with no pump power (i.e. A = B = 0) can the probe light transmit to the output port (i.e. O = 1). In other cases, the probe light is blocked (i.e. O = 0). Thus, all-optical NOR logic gate is successfully built. Therefore, reconfigurable logic gates could be realized by using different combinations of fibers and pump lights.

4. Conclusion

In conclusion, we have experimentally demonstrated an all-optical switch based on a fiber-chip-fiber opto-mechanical system driven by the thermal radiation. The experimental results show that the switching extinction ratios could be up to 60.7 dB with an operation bandwidth of at least 45 nm. The switching performances could be improved by fabricating the device in fully integrated chip and using grating couplers with ultra-low loss. Additionally, the fiber-chip-fiber opto-mechanical system has many other significant applications in all-optical systems, such as reconfigurable logic gates.

References

[1] K. Nozaki *et al.*, "Sub-femtojoule all-optical switching using a photonic-crystal nanocavity," *Nat. Photon.*, vol. 4, no. 7, pp. 477–483, 2010.

[2] T. Tanabe, M. Notomi, S. Mitsugi, A. Shinya, and E. Kuramochi, "Fast bistable all-optical switch and memory on a silicon photonic crystal on-chip," *Opt. Lett.*, vol. 30, no. 19, pp. 2575–2577, 2005.

[3] W. Chen *et al.*, "All-optical switch and transistor gated by one stored photon," *Science*, vol. 341, pp. 768–770, 2013.

[4] M. Bajcsy *et al.*, "Efficient all-optical switching using slow light within a hollow fiber," *Phys. Rev. Lett.*, vol. 102, no. 20, p. 203902, 2009.

[5] J. H. Wu *et al.*, "Ultrafast all optical switching via tunable Fano interference," *Phys. Rev. Lett.*, vol. 95, no. 5, pp. 057401, 2005.

[6] G. I. Papadimitriou, C. Papazoglou, and A. S. Pomportsis, "Optical switching: Switch fabrics, techniques, and architectures," *J. Lightw. Technol.*, vol. 21, no. 2, pp. 384–405, Feb. 2003.

[7] B. Lynn *et al.*, "Design and preliminary implementation of an N × N diffractive all-optical fiber optic switch," *J. Lightw. Technol.*, vol. 31, no. 24, pp. 4016–4021, Dec. 15, 2013.

[8] M. S. Kang, A. Butsch, and P. S. J. Russell, "Reconfigurable light-driven opto-acoustic isolators in photonic crystal fiber," *Nat. Photon.*, vol. 5, no. 9, pp. 549–553, 2011.

[9] X. Feng, H. Y. Tam, and P. K. A. Wai, "Stable and uniform multiwavelength erbium-doped fiber laser using nonlinear polarization rotation," *Opt. Exp.*, vol. 14, no. 18, pp. 8205–8210, 2006.

[10] C. Ito and J. C. Cartledge, "Polarization independent all-optical 3R regeneration based on the Kerr effect in highly nonlinear fiber and offset spectral slicing," *IEEE J. Sel. Topics Quantum Electron.*, vol. 14, no. 3, pp. 616–624, May/Jun. 2008.

[11] P. Wang *et al.*, "Multi-wavelength Erbium-doped fiber laser based on four-wave-mixing effect in single mode fiber and high nonlinear fiber," *Opt. Exp.*, vol. 21, no. 10, pp. 12570–12578, 2013.

[12] P. Hölzer *et al.*, "Femtosecond nonlinear fiber optics in the ionization regime," *Phys. Rev. Lett.*, vol. 107, no. 20, p. 203901, 2011.

[13] Y. Wang *et al.*, "Optical switch based on a fluid-filled photonic crystal fiber Bragg grating," *Opt. Lett.*, vol. 34, no. 23, pp. 3683–3685, 2009.

[14] J. Yu, R. Feng, and W. She, "Low-power all-optical switch based on the bend effect of a nm fiber taper driven by outgoing light," *Opt. Exp.*, vol. 17, no. 6, pp. 4640–4645, 2009.

[15] N. Nishizawa, Y. Ukai, and T. Goto, "Ultrafast all optical switching using pulse trapping in birefringent fibers," *Opt. Exp.*, vol. 13, no. 20, pp. 8128–8135, 2005.

[16] J. Parra-Cetina, A. Kumpera, M. Karlsson, and P. A. Andrekson, "Phase-sensitive fiber-based parametric all-optical switch," *Opt. Exp.*, vol. 23, no. 26, pp. 33426–33436, 2015.

[17] G. ttini, G. Meloni, A. Bogoni, and L. Poti, "All-optical 2×2 switch based on Kerr effect in highly nonlinear fiber for ultrafast applications," *IEEE Photon. Technol. Lett.*, vol. 18, no. 23, pp. 2439–2441, Dec. 1, 2006.

[18] Z. G. Zang and W. X. Yang, "Theoretical and experimental investigation of all-optical switching based on cascaded LPFGs separated by an erbium-doped fiber," *J. Appl. Phys.*, vol. 109, no. 10, p. 103106, 2011.

[19] Z. Zang and Y. Zhang, "Analysis of optical switching in a Yb 3+-doped fiber Bragg grating by using self-phase modulation and cross-phase modulation," *Appl. Opt.*, vol. 51, no. 16, pp. 3424–3430, 2012.

[20] P. Petropoulos *et al.*, "2R-regenerative all-optical switch based on a highly nonlinear holey fiber," *Opt. Lett.*, vol. 26, no. 16, pp. 1233–1235, 2001.

[21] J. E. Heebner and R. W. Boyd, "Enhanced all-optical switching by use of a nonlinear fiber ring resonator," *Opt. Lett.*, vol. 24, no. 12, pp. 847–849, 1999.

[22] S. R. Friberg, Y. Silberberg, M. Oliver, M. J. Andrejco, and M. A. Saifi, "Ultrafast all-optical switching in a dual-core fiber nonlinear coupler," *Appl. Phys. Lett.*, vol. 51, pp. 1135–1137, 1987.

[23] M. Asobe, T. Kanamori, and K. I. Kubodera, "Applications of highly nonlinear chalcogenide glass fibers in ultrafast all-optical switches," *IEEE J. Quantum Electron.*, vol. 29, no. 8, pp. 2325–2333, Aug. 1993.

[24] K. Suzuki *et al.*, "Ultra-high-extinction-ratio 2 × 2 silicon optical switch with variable splitter," *Opt. Exp.*, vol. 23, pp. 9086–9092, 2015.

[25] S. Han, T. J. Seok, N. Quack, B.-W. Yoo, and M. C. Wu, "Large-scale silicon photonic switches with movable directional couplers," *Optica*, vol. 2, pp. 370–375, 2015.

[26] A. Narayanaswamy, S. Shen, and G. Chen, "Near-field radiative heat transfer between a sphere and a substrate," *Phys. Rev. B*, vol. 78, no. 11, p. 115303, 2008.

[27] A. Narayanaswamy, and G. Chen, "Thermal near-field radiative transfer between two spheres," *Phys. Rev. B*, vol. 77, no. 7, p. 075125, 2008.

[28] G. Bimonte, "Scattering approach to Casimir forces and radiative heat transfer for nanostructured surfaces out of thermal equilibrium," *Phys. Rev. A*, vol. 80, no. 4, p. 042102, 2009.

[29] S. Gigan *et al.*, "Self-cooling of a micromirror by radiation pressure," *Nature*, vol. 444, no. 7115, pp. 67–70, 2006.

[30] A. I. Volokitin, and B. N. J. Persson, "Theory of the interaction forces and the radiative heat transfer between moving bodies," *Phys. Rev. B*, vol. 78, no. 15, p. 155437, 2008.

[31] H. Cai *et al.*, "A nanoelectromechanical systems optical switch driven by optical gradient force," *Appl. Phys. Lett.*, vol. 102, no. 2, p. 023103, 2013.

[32] B. Dong *et al.*, "A silicon-nanowire memory driven by optical gradient force induced bistability," *Appl. Phys. Lett.*, vol. 107, no. 26, pp. 261111, 2015.

[33] M. L. Povinelli *et al.*, "Evanescent-wave bonding between optical waveguides," *Opt. Lett.*, vol. 30, no. 22, pp. 3042–3044, 2005.

[34] S. Manipatruni, J. T. Robinson, and M. Lipson, "Optical nonreciprocity in optomechanical structures," *Phys. Rev. Lett.*, vol. 102, no. 21, p. 213903, 2009.

[35] E. S. Shuman, J. F. Barry, D. R. Glenn, and D. DeMille, "Radiative force from optical cycling on a diatomic molecule," *Phys. Rev. Lett.*, vol. 103, no. 22, p. 223001, 2009.

[36] S. B. Wang, and C. T. Chan, "Lateral optical force on chiral particles near a surface," *Nat. Commun.*, vol. 5, p. 3307, 2014.

[37] P. G. Datskos *et al.*, "Remote infrared radiation detection using piezoresistive microcantilevers," *Appl. Phys. Lett.*, vol. 69, no. 20, pp. 2986–2988, 1996.

[38] P. G. Datskos, S. Rajic, and I. Datskou, "Photoinduced and thermal stress in silicon microcantilevers," *Appl. Phys. Lett.*, vol. 73, no. 16, pp. 2319–2321, 1998.

[39] B. Kwon, M. Rosenberger, R. Bhargava, D. G. Cahill, and W. P. King, "Dynamic thermomechanical response of bimaterial microcantilevers to periodic heating by infrared radiation," *Rev. Sci. Instrum.*, vol. 83, no. 1, p. 015003, 2012.

[40] J. L. Corbeil, N. V. Lavrik, S. Rajic, and P. G. Datskos, "Self-leveling" uncooled microcantilever thermal detector," *Appl. Phys. Lett.*, vol. 81, no. 7, pp. 1306–1308, 2002.

[41] E. A. Wachter *et al.*, "Remote optical detection using microcantilevers," *Rev. Sci. Instrum.*, vol. 67, no. 10, pp. 3434–3439, 1996.

[42] P. G. Datskos, N. V. Lavrik, and S. Rajic, "Performance of uncooled microcantilever thermal detectors," *Rev. Sci. Instrum.*, vol. 75, no. 4, pp. 1134–1148, 2004.

[43] N. V. Lavrik, M. J. Sepaniak, and P. G. Datskos, "Cantilever transducers as a platform for chemical and biological sensors," *Rev. Sci. Instrum.*, vol. 75, no. 7, pp. 2229–2253, 2004.

[44] L. Liu *et al.*, "Low power consumption and continuously tunable all-optical microwave filter based on an opto-mechanical microring resonator," *Opt. Exp.*, vol. 25, no. 2, pp. 960–971, 2017.

[45] D. Van Thourhout and J. Roels, "Optomechanical device actuation through the optical gradient force," *Nat. Photon.*, vol. 4, no. 4, pp. 211–217, 2010.

[46] M. Li *et al.*, "Harnessing optical forces in integrated photonic circuits," *Nature*, vol. 456, no. 7221, pp. 480–484, 2008.

[47] Y. Ding, C. Peucheret, H. Ou, and K. Yvind, "Fully etched apodized grating coupler on the SOI platform with −0.58 dB coupling efficiency," *Opt. Lett.*, vol. 39, no. 18, pp. 5348–5350, 2014.